Polymer 51 (2010) 2683–2689

Contents lists available at ScienceDirect

Polymer

journal homepage: www.elsevier.com/locate/polymer

Fabrication of polymer antireflective coatings by self-assembly of supramolecular block copolymer

Junpeng Gao, Xiao Li, Binyao Li, Yanchun Han*

Chinese Academy of Sciences, Graduate School of the Chinese Academy of Sciences, State Key Laboratory of Polymer Physics and Chemistry, Changchun Institute of Applied Chemistry, 5625 Renmin Street, Changchun 130022, PR China

ARTICLE INFO

Article history:
Received 26 July 2009
Received in revised form
4 December 2009
Accepted 22 March 2010
Available online 8 April 2010

Keywords:
Supramolecular self-assembly
Broadband antireflection
Hydrogen bonding

ABSTRACT

We demonstrated a method of fabricating antireflective coatings based on the self-assembly of supramolecular block copolymer formed by polystyrene terminated with carboxyl (PS-COOH) and poly(methyl methacrylate) terminated with amine (PMMA-NH_2) via hydrogen bonding. Different porous films were generated by selectively removing PS-COOH from the spin-coated films with a selective solvent, cyclohexane, under different conditions. The refractive index of such porous film can be tuned from 1.49 down to 1.26 by controlling the thickness of the porous film. For the porous layer with $n \sim 1.26$, the light transmittance of the glass about 97.93% was achieved in the visible range ($\lambda \sim 574$ nm). By varying the solution concentration and exposing time in cyclohexane, inhomogeneous three-layered porous films were generated: top and bottom layers with high porosities and the middle layers with lower porosities, respectively. The light transmittance of the glass coated with this inhomogeneous film was about 98.00% in the near-infrared region corresponding to wavelength between 800 and 1400 nm. The wavelength region of the broadband antireflective films with high transmittance more than 99.00% can be fine tuned to 1200–2000 nm with increasing the film thickness.

1. Introduction

Since the light reflection of glass surfaces is undesirable, disturbing, and limits the performance of devices [1], antireflective coatings play an important role in a wide variety of optical technologies by reducing reflective losses at interfaces [2]. They have been widely used in many applications, such as flat-panel displays, solar cells, lasers and other optical-electronic devices [3–5]. The basic principle of antireflective coating is destructive interference of the reflected light from air-coating and coating-substrate interfaces [6]. For ideal homogeneous single-layer antireflective coating, two conditions should be met: the optical thickness of the coating must be 1/4 of the wavelength of the incident light; $n_f = (n_o n_s)^{1/2}$, where n_f, n_o, n_s, is the refractive index of film, air, and substrate, respectively. Since the refractive indices of glass and transparent plastic substrates are generally about 1.52, the refractive index of the antireflection coating should be 1.23 to meet complete zero reflectance at a specific wavelength. However, single antireflective coating cannot satisfy this condition, because the lowest refractive index of homogeneous dielectric material is about 1.35 [6]. One approach to lower the refractive index is to design nanoporous structure and maintain that the homogeneously distributed pore sizes are smaller than the wavelengths of incidence light. Such materials can possess a very low effective n (given by an average over the film) due to the introduction of air [7], which has the lowest refractive index of 1.00.

Various top-down and bottom-up techniques have been proposed to make thin films with tunable porosity. Using chemical etching method, the transparent substrates can be roughened by leaching out materials from their surfaces to produce small pores [8–10]. Sol–gel technique [11–14] is one of the widely used techniques for the forming of porous coatings, and the pore size can be modified by tuning the process parameters. The deposition of inorganic or organic charged colloidal particles on glass substrates by electrostatic interaction has been carried out to obtain antireflective coatings [15–21]. Recently, Kotov prepared an antireflective film using the stiff and rigid tunicate cellulose nanowires by layer-by-layer (L-B-L) assembly [22]. In nature, the moth's eye structure is an excellent antireflective coating [23]. Based on the layer-by-layer assembly method [24] a snowman-like arrays of colloidal dimmers by alternating layers of charged polymer colloids and polyeletrolytes (PE), were fabricated as a moth-eye-like structure with a gradient-refractive-index [18]. Compared with the inorganic materials, polymer materials have been widely used for antireflective coating because of easy and economic processing. Based on

* Corresponding author. Tel.: +86 431 85262175; fax: +86 431 85262126.
E-mail address: ychan@ciac.jl.cn (Y. Han).

0032-3861/$ – see front matter © 2010 Published by Elsevier Ltd.
doi:10.1016/j.polymer.2010.03.035

the microphase separation, an antireflective coating with nanoporous structure was obtained from the self-assembled polymer blends or block copolymer film followed by selectively removing one block [25]. Making use of different evaporation speed of solvents, an antireflective coating with a solid skin layer and an inner porous layer was formed by spin-coating polymer/solvent/nonsolvent ternary system on glass substrate [26]. Char and coworkers prepared the antireflective coatings of block copolymer micelles (BCM) films, which were assembled making using of the electrostatic and hydrogen-bonding interactions between different BCMs [20].

However, the main disadvantage of the antireflective coating is that the high transmittance is only at the narrow wavelength region, and the application is limited. To achieve broadband antireflection properties, it is necessary to create a film with gradient-refractive-index, which index increases gradually from the top to the bottom of the film [1,27,28]. Surface possessing a gradient-refractive-index over sufficient depth, such as the cornea of the moth's eye, show minimized reflection over a broad range of wavelengths and angles of incidence [2]. In addition, due to the important application in near-infrared region, antireflective coating has been used in transmitting optics, for example, output couplers, dichroic mirrors, lenses, and windows to eliminate light reflection from an antireflective spin-coating surface where the signals or energy of light is received [30,31]. However, to our knowledge, there are few papers reported on the fabrication of broadband antireflective coatings with simple method at near-infrared wavelengths, and the methods always need several steps [32,2,29]. Also, it would be much more interesting to control the region of wavelengths to meet practical applications.

Here, we present a new procedure for creating porous polymer films based on the self-assembly of supramolecular block copolymer for antireflective coatings. The self-assembly behavior of supramolecular block copolymer, which is a A–B type diblock copolymer that relies on hydrogen-bonded-enforced association of incompatible polymer chains, is similar with the block copolymer that the two blocks are connected by covalent bond. Due to the weakness of hydrogen bonding, one component can be easily removed with a selective solvent to create a porous film. The structure of the film formed by supramolecular block copolymer is generally nanoscale in size, ranging from 5 to 100 nm, which are much smaller than the wavelengths of incident light to prevent the light scattering. The porous films with various thicknesses showed high transmittance at specific wavelength in visible lights and broadband antireflective property in near-infrared region. Different from the broadband antireflective coatings of bilayers or multilayers that were fabricated step by step, in this case, inhomogeneous three-layered structures with different pore volume fraction in porous films can be obtained with one step, and the broadband antireflective properties could be achieved. To meet more applications, the broadband region can be tuned by controlling the thickness of the porous film.

2. Experimental section

2.1. Materials

The homopolymers with functional terminated groups, polystyrene terminated with carboxyl (PS-COOH, Mw = 10 500, Mw/Mn = 1.05) and poly(methyl methacrylate) terminated with amide (PMMA-NH_2, Mw = 9720, Mw/Mn = 1.13), were supplied by Polymer Source, Inc., and used as received. Tetrahydrofuran and cyclohexane (A. R. grade) was supplied by Beijing Chemical Reagent Co., and used without purification. Deionized (DI) water was obtained using the Millipore water purification system. All glassware were washed with piranha solution (H_2SO_4:H_2O_2 (7:3) *hazardous* solution!) by sonication for 30 min in a normal ultrasonic bath (50 Hz) and was rinsed thoroughly with DI water. Glass slides with 1.20 mm thick were purchased from Nanbo group, China, and the refractive index is 1.52. The glass was cleaned by dipping in the mixture of sodium hydroxide and ethanol and sonicated for 30 min. Subsequently, the substrates were rinsed repeatedly with DI water and blown dry in a N_2 flow.

2.2. Sample preparation

The solutions containing the two homopolymers were prepared by mixing PS-COOH and PMMA-NH_2 with equal mol ratio in tetrahydrofuran with a desired concentration and stirred for 72 h by a magnetic stirrer at room temperature. The samples were prepared by spin-coating the solutions onto the freshly cleaned glass slides. The spin-coating speed was kept at 3000 rpm for all samples using a commercial spin-coater KW-4A, Chemat Technology Inc. After removing residual solvent in spin-coated films in a vacuum for 48 h, the PS-COOH components were removed by exposing the samples for different times in cyclohexane without stirring. All the samples were finally dried at room temperature in a vacuum for 48 h to remove any residual solvent. Prior to SEM test, the sample was put into liquid nitrogen for several seconds. The substrates were broken from the surface scratch marks. The cross-section was used in SEM test.

2.3. Characterization

The morphologies of the obtained products were investigated by atomic force microscopy (AFM). AFM was performed on a commercial scanning probe microscopy (SPA 300HV with an SPI 3800 N probe station, Seiko Instruments Inc., Japan) in tapping mode. A silicon microcantilever (spring constant 2 N m^{-1} and resonance frequency 70 kHz, Olympus, Japan) with an etched conical tip (radius of curvature 40 nm as characterized by scanning over very sharp needle array, NT-MDT, Russia) was used for scan.

The cross-sectional micrographs of all the samples were investigated by a Micro FEI PHILIPS XL-30-ESEM-FEG field emission scanning electronic microscope (FESEM) operating at 20 kV. The samples for scanning electron microscopy were coated with a 20–30 Å layer of Au to make them conductive.

Coating transmittance of normally incident light was measured using a UV–vis spectrophotometer, UV-3600, SHIMADZU, over the spectral range of 400–2000 nm. A custom sample holder was used.

Film thicknesses and refractive indices of porous films were determined by an ellipsometry (AUEL-III, Xi'an, China). The film thicknesses were also measured by purposely applying a scratch to the polymer film and subsequent AFM imaging in the vicinity of the scratch.

3. Results and discussion

3.1. Structure of porous films after removing PS-COOH from the spin-coated films

The model system in this work consisted of a binary polymer blend of mono-end-carboxyled polystyrene (PS-COOH) and mono-end-aminated polymethyl methacrylate (PMMA-NH_2). A pictorial representation of the blend system was given in Scheme 1. As shown in Scheme 1, mixing the two polymers with a mol ratio of 1:1 in a common solvent (tetrahydrofuran) should lead to hydrogen-bonded supramolecular diblock copolymer. The morphology of such blend was basically governed by the competition between two types of interactions: the unfavorable

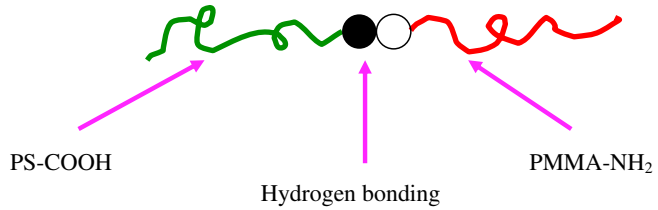

Scheme 1. Schematic representation of the supramolecular block copolymer formed by PS-COOH and PMMA-NH_2 via hydrogen bonding. The filled circles and the open circles represent the carboxyl group and amine group, respectively.

interaction between dissimilar polymers, and the specifically attractive interaction between two different functional groups attached to each of the chain ends of dissimilar polymers [33]. So the phase behavior of this kind of supramolecule was similar with the typical diblock copolymers [33–36]. The microphase separation was confirmed by the AFM images of their spin-coated films from the solution containing PS-COOH and PMMA-NH_2 (Fig. 1). The concentrations of the solution were fixed at 1.00 wt%, 2.00 wt%, 3.00 wt%, 4.00 wt%, and the corresponding thicknesses of the films were 50 nm, 104 nm, 152 nm, 203 nm, respectively. The weight averaged molecular weight of PS-COOH and PMMA-NH_2 is 10 500 and 9720, respectively, and the volume fraction ratio between PS-COOH and PMMA-NH_2 is 0.55/0.45. So the lamellar microdomains in the equilibrium state should be expected [37]. However, randomly distributed nanodomains were observed without exhibiting a sharp boundary between PS-COOH and PMMA-NH_2 blocks. The reason was that the morphology obtained by spin-coating was far from equilibrium morphology since the evaporation rate of tetrahydrofuran was very fast. The polymer chains had not enough time to reach the kinetics equilibrium state so that the lamellar morphology was obtained, which was the same as the morphology after annealing at high temperatures [38].

Porous structure can be generated by selectively removing one component from the phase-separated film formed by block copolymers [37]. But the treatment of ultra-violet irradiation or ozone is needed to destroy the covalent among one of the blocks. As known, the strength of noncovalent is much weaker than that of covalent, and can be tuned by stimuli, such as temperature [14] and selective solvent exposing [39]. In this case, the porous films can be generated one step by exposing the spin-coated films in a selective solvent, cyclohexane, to remove the component of PS-COOH [40,41], while PMMA-NH_2 remained due to its poor solubility in cyclohexane.

Because the size of microdomains generated from the self-assembly of supramolecular block copolymer in this case was nanoscale, it was reasonable that the pores in the films after selectively removing the microdomains formed by PS-COOH were also nanoscale. However, for the spin-coated film with 50 nm, at the exposing time of 5 min (Fig. 2a), both nanopores and micropores were obtained. With increasing the exposing time from 5 min to 10–40 min (Fig. 2b–e), the microporous films without nanopores were obtained. All the experiments suggested that the release of PS-COOH should not be directly responsible for the formation of the micropores with about 1 μm, because the microdomains formed by PS-COOH are nanoscale (Fig. 1a). Therefore, it was reasonable to think that the micropores were a result of the reconformation of PMMA-NH_2 induced by cyclohexane [42]. Although cyclohexane is a nonsolvent for PMMA, due to the plasticizing effect, the Tg of PMMA decreased and the mobility of PMMA chains increased, which caused the PMMA domains to merge to reduce surface energy. Thus, the pore size and film thickness increased. Actually, the film thicknesses were increased from 50 nm to 56 nm after 10 to 40 min exposing time.

However, for the spin-coated films with 104 nm, 152 nm and 203 nm, lateral structures larger than 100 nm were absent and a rough surface without individual pores was obtained after exposing the spin-coated films in cyclohexane for 5–40 min (Fig. 2f–j (104 nm); Fig. 2k–o (152 nm); Fig. 2p–t (203 nm)). The reason may be that it was difficult to induce the rearrangement of the films with increasing film thickness. Similar with the results obtained from the spin-coated film with 50 nm, the film thickness was almost not changed after exposing the spin-coated films in cyclohexane for 5 min. With increasing the exposing time, the thickness of the porous films was also increased.

To investigate the inner structure of the porous films, the cross-sectional structure of the porous films after exposing the spin-coated films with 152 nm in cyclohexane for different times was characterized by FESEM (Fig. 3a–e). At the exposing time of 5 min, there were little pores in the film. With increasing the exposing time to 10 min, more pores could be obtained. As the exposing time was increased to 20 min, 30 min and 40 min, inhomogeneous porous structures were obtained. A kind of inhomogeneous three-layered structure was obtained with some pores in the top and bottom layer, and a relative compact structure in the middle layer. It is the solvent evaporation rate that controlled the hydrogen-bonded supramolecular diblock copolymer nanostructures [43–46]. After the film was taken from cyclohexane, the concentration of cyclohexane at the surface was the lowest and a gradient concentration developed throughout the vertical direction of the film [47]. With the solvent evaporation, phase separation between the polymer and cyclohexane occurred only at the surface, which resulted in the gradient structure after the release of PS-COOH. Compared with the fast phase separation between polymer and cyclohexane at surface, it was slow within the film, because the evaporation speed of cyclohexane is slow, which resulted in the relative compact

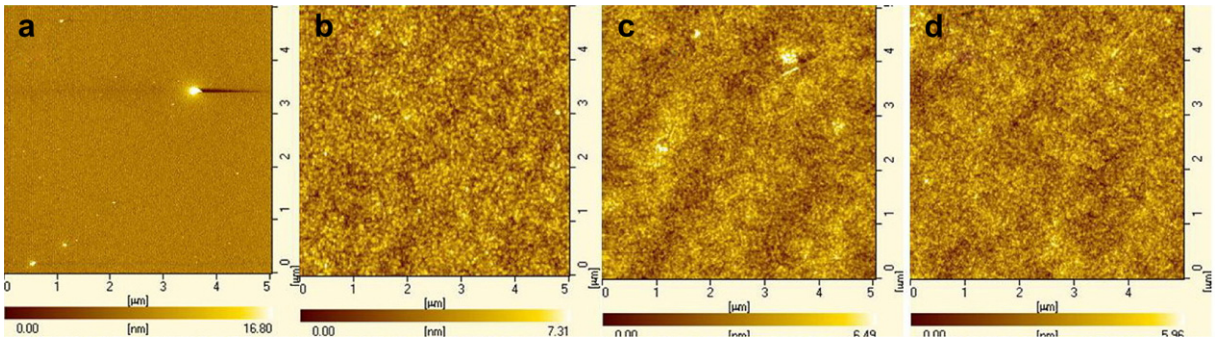

Fig. 1. AFM images of the films spin-coated from the solution containing PS-COOH and PMMA-NH_2 with different concentrations: (a) 1.00 wt%, (b) 2.00 wt%, (c) 3.00 wt% and (d) 4.00 wt%. The mol ratio of the two homopolymers was fixed at 1:1.

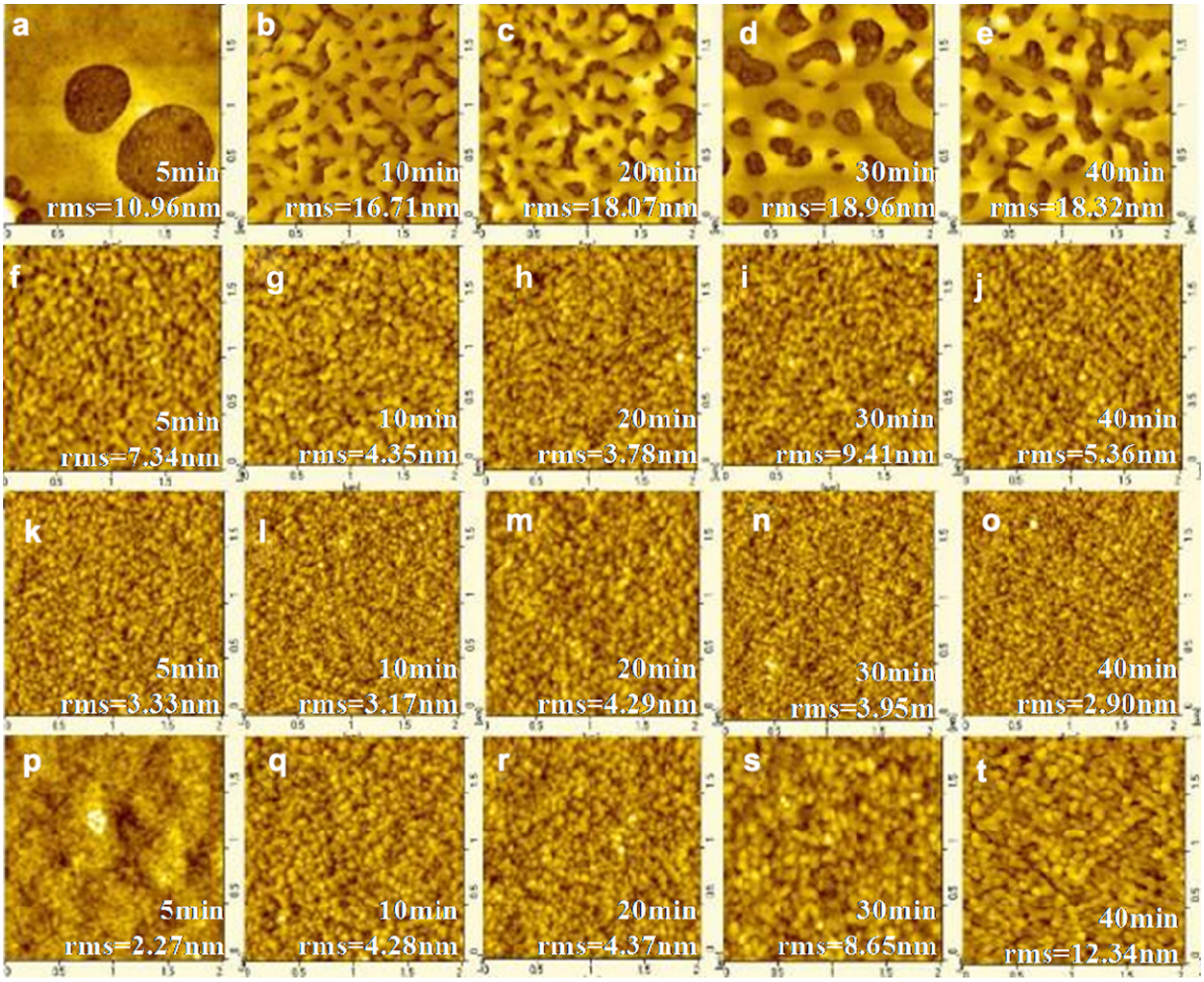

Fig. 2. AFM images of the porous films after removing the component of PS-COOH by exposing the films in cyclohexane for 5–40 min. The thickness of the original spin-coated films was (a–e) 50 nm, (f–j) 104 nm, (k–o) 152 nm, and (p–t) 203 nm, and surface roughness of the porous films was also showed in each image.

structure in the middle layer. In addition, to reduce the contact area between slight hydrophobic PMMA-NH_2 and hydrophilic surface of glass, the extended PMMA-NH_2 chains in bottom layer gradually folded and the coverage in lateral direction decreased, resulted in the formation of pores in the bottom layer. In the case of the spin-coated film with 203 nm (Fig. 3f–j), porous structures were similar with the case of porous films generated from the spin-coated films with 152 nm.

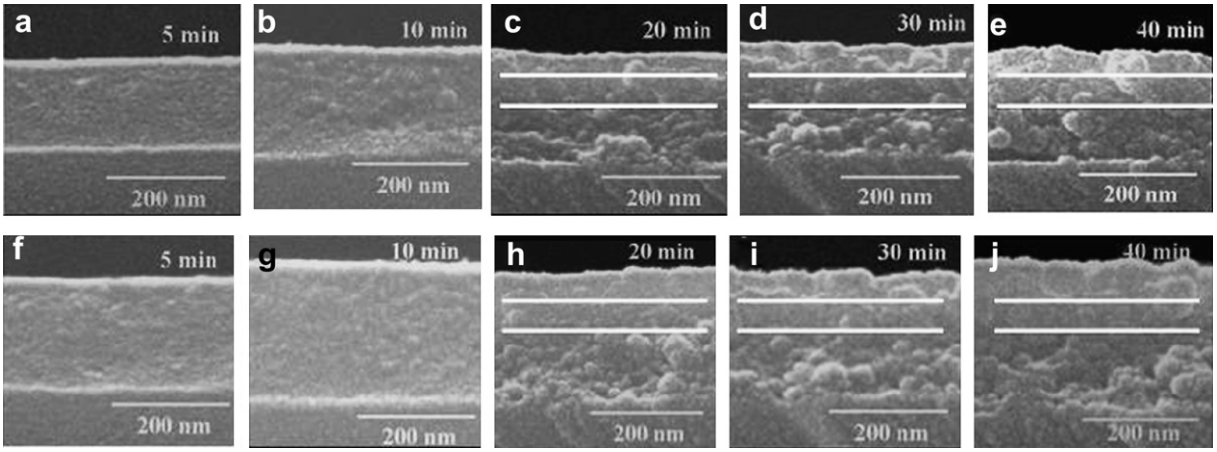

Fig. 3. FESEM images of the porous films after removing the component of PS-COOH by exposing the films in cyclohexane for 5–40 min. The thickness of the original spin-coated films was (a–e) 152 nm, (f–j) 203 nm.

3.2. Antireflective property of the porous films

Since the porous films can be generated by selectively removing the component of PS-COOH, it was reasonable that the optical property of the films would be changed. The transmission of the glass slides covered with porous films (after exposing the spin-coated films in cyclohexane for 5–40 min) on both slides was shown in Fig. 4. For comparison, the transmission of an uncoated glass slide and the original spin-coated films were also shown.

For the original spin-coated film with 50 nm, the transmittance was slightly decreased to 88.82% at 400 nm, compared with an uncoated glass slide, 89.39%, (Fig. 4a). After exposing the film in cyclohexane for 5 min, the transmittance was increased to 93.36% at 400 nm. As the exposing time was increased to 10 min, 20 min and 30 min, the maximum transmittance loadings became 93.63%, 94.02% and 94.47% at 400 nm, respectively. The maximum transmittance of 95.06% was achieved when the exposing time was increased to 40 min.

For the original spin-coated film with 104 nm, the transmittance was only 89.93% at 535 nm (Fig. 4b). After exposing the film in cyclohexane for 5 min, the transmittance was increased by 4.69% at 535 nm to 93.62%, compared with the transmittance of uncoated glass, 89.93%. As the exposing time in cyclohexane was increased to 10 min and 20 min, the maximum transmittance of glasses coated with porous films loadings became 97.65% and 97.93% at 574 nm, respectively. With continuously increasing the exposing time in cyclohexane to 30 min and 40 min, the transmittance decreased slightly, and reached to 96.48% and 96.95% at 582 nm, respectively.

For the porous films with inhomogeneous three-layered structures, broadband antireflection at the near-infrared region of 800–1400 nm was achieved (Fig. 4c (the original spin-coated film was 152 nm)), while the original spin-coated film showed low transmittance with no more than 88.00%. After exposing the film in cyclohexane for 5 min and 10 min, the average transmittance at this wavelength region was increased to 92.00% and 95.00%, while the transmittance of uncoated glass in this region was only 90.00%. As the exposing time in cyclohexane was increased to 20 min, 30 min and 40 min, the average transmittance of glasses coated with porous films loadings became about 97.00%, 97.50% and 97.20% at 800–1400 nm respectively.

For the spin-coated film with further increased thickness of 203 nm, after exposing for 5–40 min, the broadband antireflective properties were also obtained (Fig. 4d), while the wavelength range was moved from 800–1400 nm to 1200–2000 nm. UV–vis characterization revealed linearly increasing transmittance at this region by increasing the exposing time from 5 to 30 min (Fig. 4d). At the exposing time of 5 and 10 min, the transmittances were both not more than 95.00%. As increasing the exposing time to 20 min and 30 min, the high transmittance at 1200–2000 nm can be reached to about 98.50% and 99.00%, respectively. However, the transmittance of the porous film after 40 min exposing decreased largely.

3.3. Relationship between the structure and the antireflective property of porous films

For antireflective coatings, the pore volume fraction of the film determines the final refractive index. As mentioned above, for zero reflectance, refractive index of the porous film coated on the glass should be 1.23. Under this condition, the optimum pore volume fraction in the film with zero reflectance can be estimated according to Ref. [48],

$$n^2 = n^2_{\text{polymer}}\left(1 - f_{\text{pore}}\right) + n^2_{\text{air}}\, f_{\text{pore}} \tag{1}$$

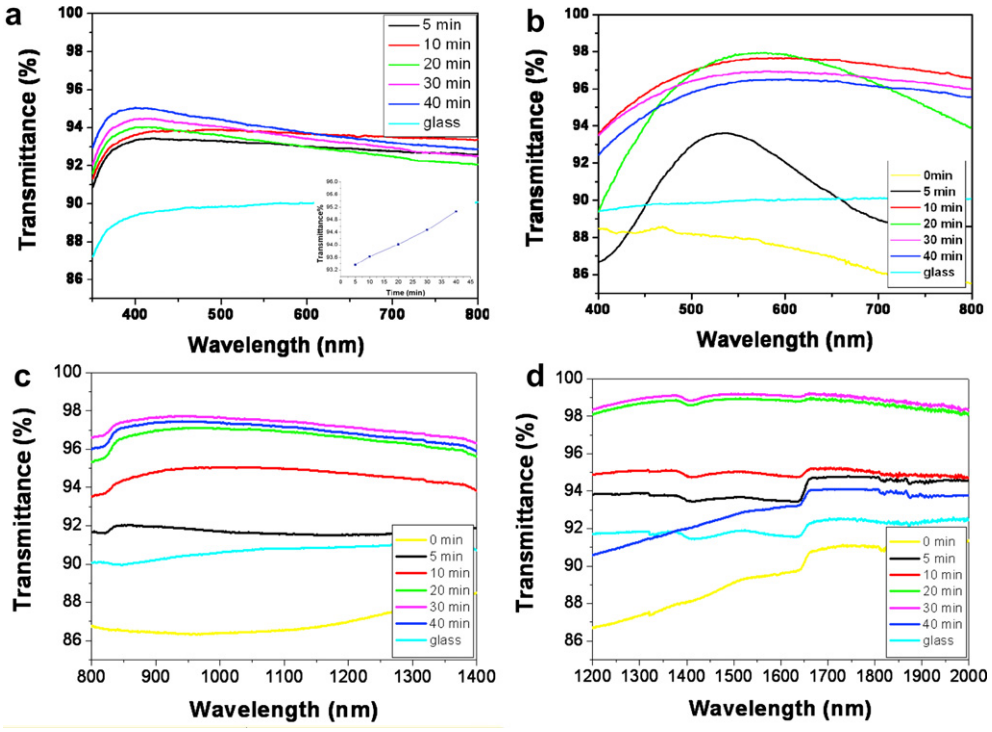

Fig. 4. The corresponding UV–vis transmittance for the glasses coated with the porous films on both slides after exposing the spin-coated films in cyclohexane for 5–40 min. The thickness of the original spin-coated films was (a) 50 nm (inset figure: The linearly increasing light transmittance at 400 nm with increasing the exposing time in cyclohexane.), (b) 104 nm, (c) 152 nm, and (d) 203 nm.

where $n_{polymer}$, n_{air} and f_{pore} are the refractive index of polymer, air and the pore volume fraction of the film, respectively. The refractive index of the polymer of PMMA and air is 1.49 and 1.00, respectively. Thus, to obtain zero reflectance, the pore volume fraction of the film should be 57.96%. In this case, after selectively removing all the component of PS-COOH, the pore volume fraction of the porous films is 54.76%, and the corresponding n of the film is 1.25 according to the formula (1), which is enough to achieve the high transmittance more than 99.00% [1].

For the porous films created by exposing the spin-coated film with 50 nm in cyclohexane for 5–40 min, the average refractive index of the films was about 1.24. According to the formula (1), the average volume fraction of the porous films was about 67.28%, which was higher than the theoretic value, 54.76%. The reason may be that more pores were generated due to the rearrangement of the films by exposing the films in cyclohexane. Although UV–vis characterization revealed linearly increasing light transmittance at 400 nm with increasing the exposing time in cyclohexane (Fig. 4a), the average transmittance and the maximum of transmittance of the coatings was only about 94.00% and 95.06% at 400 nm, respectively. Except for the refractive index, surface topography of the films also had a big effect on the transmittance and can lead to surface scattering to reduce the transmittance intensity. Optical transmission through a rough surface is considerably affected by scattering of light [14]. To quantify the surface topography of the porous films fabricated in this case, the root-mean-square (rms) surface roughness of the porous films was less than 20 nm as shown in Fig. 2a–e, which was small enough not to cause any intense surface light scattering as long as the wavelength is no longer than 200 nm [49]. But, why the maximum transmission of the coatings with low refractive indices (around 1.24) was only 95.06%? As mentioned above, the thickness of the coating must be 1/4 of the wavelength of the incident light. Thus, to achieve high transmittance in visible wavelengths, the coating thickness should be located in the area of 80–200 nm. However, the thickness of the porous films was only about 56 nm after exposing the spin-coated film in cyclohexane for 20–40 min, which was too thin to satisfy the $\lambda/4$ requirement for the maximum transmittance of 400 nm. Thus, it was reasonable that the coating cannot reach high transmittance in visible wavelengths, whatever the exposing time was.

For the original spin-coated film with 104 nm, the thickness satisfied the requirement of maximum transmittance in visible lights. After exposing the film in cyclohexane for 5 min, the pore volume fraction of the film was 21.32%. Since the pore volume fraction of the porous films was 54.76% after selectively removing all the component of PS-COOH, it was reasonable to think that the PS-COOH components in this film were not removed completely with short exposing time of 5 min. The film thickness was nearly not changed and refractive index of this porous film was 1.38. Thus, the transmittance was increased only by 4.69% at 535 nm to 93.62%. As the exposing time in cyclohexane was increased to 10 min and 20 min, more chains of PS-COOH that hydrogen-bonded to PMMA-NH_2 were released from the film by increasing the exposing time which resulted in the high pore volume fractions dramatically increasing to 49.76%. The refractive indices were also decreased to about 1.26. Accordingly, the maximum transmittances of glasses coated with porous films were dramatically increased to 97.65% and 97.93% for the films with 10 min and 20 min exposing time, respectively. However, the maximum transmittance wavelength was moved from 535 nm to 574 nm, as shown in Fig. 4b. This result indicated that the thicknesses of the films were increased by 12–116 nm compared to the film with 5 min exposing time. With continuously increasing the exposing time in cyclohexane to 30 min and 40 min, the PMMA-NH_2 chains merged continuously, and the thickness was also increased, resulted in the red-shifted to 582 nm of the maximum transmittance wavelength. In fact, the film thicknesses were increased about 2–118 nm. However, the pore volume fractions of the films were slightly decreased to about 47.60% and the refractive indices were increased to about 1.28. The slight decrease of pore volume fraction in the films may be induced by the reconformation of PMMA-NH_2 chains, resulted in the slight decrease of transmittance (96.48% for 30 min exposing, and 96.95% for 40 min exposing). However, the maximum pore volume fraction of these porous films was 49.76%, and less than 54.76% that was obtained in theory. The reason may be that the long exposing time led to the rearrangement of films.

For the spin-coated film with 152 nm, after exposing the film in cyclohexane for 5 min, the pore volume fraction and refractive index of the film was 16.70% and 1.42, respectively. The average transmittance at 800–1400 nm (Fig. 4c) was only increased by about 1.00–91.50%. The film thickness was nearly not changed under this condition. As the exposing time in cyclohexane was increased to 10 min, the film thickness was slightly increased to 167 nm due to the reconformation of PMMA-NH_2 chains. The pore volume fraction was increased from 16.70% to 36.98%, and the refractive index was down to 1.33. Accordingly, the average transmittance at 800–1400 nm of glasses coated with porous films was increased to 94.60%. With increasing the exposing time to 20 min and 30 min, more chains of PS-COOH that hydrogen-bonded to PMMA-NH_2 were released from the film, resulted in the high pore volume fraction, which was dramatically increased to 47.67% and 49.76%, and the refractive index was also decreased to about 1.28 and 1.27 for the films with 20 min and 30 min exposing time, respectively. The broadband high transmittances at 800–1400 nm were achieved due to the formation of inhomogeneous three-layered structures, and increased as high as 97.00% and 97.50%. Further increasing the exposing time to 40 min, the pore volume fraction and refractive index were nearly as the same as the porous film with 30 min exposing time. However, the swollen degree of polymer film was increased, resulted in the formation of structures with large size after the complete evaporation of cyclohexane. The dividing line among the three layers was not obvious, and the average transmittance was slightly decreased to 97.30%.

For the porous films generated from the spin-coated films with increased thickness of 203 nm, it was expected that the wavelength region should be red-shifted to high wavelengths. Actually, the wavelength region (Fig. 4d) was moved from 800–1400 nm to 1200–2000 nm, compared with the spectrum in Fig. 4c. At the exposing time of 5 min the volume fraction and refractive index was only 16.70% and 1.42, respectively. So the average transmittance in this region was only about 93.50%. The film thickness was nearly not changed under the condition of short exposing time. With increasing the exposing time to 10 min, although the volume fraction was increased to 28.21% and the refractive index was decreased to 1.38. The average transmittance in this region was not more than 95.00%. The film thickness was increased to about 212 nm, due to the reconformation of PMMA-NH_2 chains. At the exposing time of 20 min and 30 min, the volume fraction of the films was increased to 47.67% and 49.76%, respectively. And the refractive index was also decreased to 1.28 and 1.27, respectively. Thus, the broadband transmittance accounted for the formation of inhomogeneous three-layered structure was increased to 98.50% and 99.00% at the exposing time of 20 min and 30 min, respectively. However, the transmittance of the porous film with 40 min exposing time decreased largely. The reason may be that the rearrangement of the film was relatively high and a lot of large structures were induced. At the mean time,

Table 1
The porosity ratio, refractive index, the highest transmittance and surface roughness for different films: the concentration is (a) 1.00 wt%, (b) 2.00 wt%, (c) 3.00 wt%, (d) 4.00 wt%.

	f_{pore} (%)	n	T%	rms (nm)
(a)				
5 min	66.32	1.25	93.36	10.0
10 min	67.28	1.24	93.63	16.7
20 min	67.28	1.24	94.02	18.1
30 min	67.28	1.24	94.47	18.0
40 min	68.35	1.24	95.06	18.3
(b)				
5 min	21.32	1.40	93.62	7.5
10 min	47.67	1.27	97.65	4.4
20 min	49.76	1.27	97.93	3.8
30 min	47.67	1.28	96.48	9.4
40 min	47.67	1.28	96.95	5.4
(c)				
5 min	16.70	1.42	91.72	3.33
10 min	36.98	1.33	95.02	3.17
20 min	47.67	1.28	97.11	4.29
30 min	49.76	1.27	97.73	2.95
40 min	49.76	1.27	97.46	2.90
(d)				
5 min	16.70	1.42	93.78	2.27
10 min	47.67	1.28	95.12	4.28
20 min	47.67	1.28	98.86	4.37
30 min	49.76	1.27	99.12	8.65
40 min	47.67	1.28	91.86	12.34

the thicknesses of the porous films were also increased from 203 nm to about 245 nm. Thus, the broadband region was tuned from 800–1400 nm to 1200–2000 nm by increasing the film thicknesses. The porosity ratio, refractive index, highest transmittance and surface roughness for different films were all summarized in Table 1.

4. Conclusion

We demonstrated a method of fabricating antireflective coatings based on the self-assembly of supramolecular block copolymer formed by polystyrene terminated with carboxyl (PS-COOH) and poly(methyl methacrylate) terminated with amine (PMMA-NH_2) via hydrogen bonding. Microphase separated films in a short range scale were obtained from the self-assembly of supramolecluar block copolymer. After removing the component of PS-COOH with a selective solvent, cyclohexane, from the spin-coated films with different thicknesses, different porous structures can be obtained. The porous film with 116 nm with an appropriate exposing time of 20 min showed high transmittance of 97.93% in visible lights (~574 nm). When the thicknesses of the spin-coated films were increased to 152 nm and 203 nm, a kind of inhomogeneous three-layered structure of the top and bottom layer with high porosities and the middle layer with low porosities were generated after exposing the spin-coated films in cyclohexane for 20–40 min. These three-layered porous films coated on both slides of the glass exhibited broadband high transmittance about 98.00% and 99.00% over 800–1400 nm and 1200–2000 nm for the porous films with 186 nm and 243 nm, respectively.

Acknowledgments

This work was subsidized by the National Natural Science Foundation of China (20621401, 550773080) and the Ministry of Science and Technology of China (2009CB930603).

References

[1] Walheim S, Schaffer E, Mlynek J, Steiner U. Science 1999;283:520.
[2] Hiller J, Mendelsohn JD, Rubner MF. Nat Mater 2002;1:59.
[3] Lowdermilk WH, Milam D. Appl Phys Lett 1980;36:891.
[4] Zheng Y, Kikuchi K, Yamasaki M, Sonoi K, Uehara K. Appl Opt 1997;36:6335.
[5] Bilyalov R, Stalmans L, Poortmans J. J Electrochem Soc 2003;150:G216.
[6] Born M, Wolf E. Principles of optics: electromagnetic theory of propagation, interference, and diffraction of light. 4th ed. Oxford: Pergamon; 1970. Ch. 1.
[7] Yoldas BE. Appl Opt 1980;19:1425.
[8] Schirone L, Sotgiu G, Califano FP. Thin Solid Films 1997;297:296.
[9] Vitanov P, Kamenova M, Tyutyundzhiev N, Delibasheva M, Goranova E, Peneva M. Thin Solid Films 1997;297:299.
[10] Adamian ZN, Hakhoyan AP, Aroutiounian VM, Barseghian RS, Touryan K. Sol Energy Mater Sol Cells 2000;64:347.
[11] Biswas PK, Devi PS, Chakraborty PK, Chatterjee A, Ganguli D, Kamath MP, et al. J Mater Sci Lett 2003;22:181.
[12] Janotta M, Katzir A, Mizaikoff B. Appl Spectrosc 2003;57:823.
[13] Wu G, Wang J, Shen J, Yang T, Zhang Q, Zhou B, et al. Mater Sci Eng 2000;78:135.
[14] Vincent A, Babu S, Brinley E, Karakoti A, Deshpande S, Seal S. J Phys Chem C 2007;111:8291.
[15] Prevo BG, Hwang Y, Velev OD. Chem Mater 2005;17:3642.
[16] Hattori H. Adv Mater 2003;13:51.
[17] Zhang X, Fujishima A, Jin M, Emeline AV, Murakami TJ. Phys Chem B 2006;110:25142.
[18] Koo HY, Yi DK, Yoo SJ, Kim DY. Adv Mater 2004;16:274.
[19] Wu Z, Walish J, Nolte A, Zhai L, Cohen RE, Rubner MF. Adv Mater 2006;16:2699.
[20] Cho J, Hong J, Char K, Caruso F. J Am Chem Soc 2006;128:9935.
[21] Zhang XT, Sato O, Taguchi M, Einaga Y, Murakami T, Fujishima A. Chem Mater 2005;17:696.
[22] Podsiadlo P, Sui L, Elkasabi Y, Burgardt P, Lee J, Miryala A, et al. Langmuir 2007;23:7901.
[23] Clapham PB, Hutley MC. Nature 1973;244:281.
[24] Decher G. Science 1997;277:1232.
[25] Joo W, Park MS, Kim JK. Langmuir 2006;22:7960.
[26] Park MS, Lee Y, Kim JK. Chem Mater 2005;17:3944.
[27] Macleod HA. Thin-film optical filters. Bristol, UK: Hilger; 1986.
[28] Miont MJ. J Opt Soc Am 1976;66:515.
[29] Kim S, Cho J, Char K. Langmuir 2007;23:6737.
[30] Many commercial products related to NIR laser optics are available; see, for instance, http://www.lasercomponents.de/wwwe/index.html.
[31] Wang Y, Cheng X, Lin Z, Zhang C, Xiao H, Zhang F, et al. Mater Lett 2004;58:2261.
[32] Park MS, Kim JK. Langmuir 2005;21:11404.
[33] Huh J, Park HJ, Kim KH, Kim KH, Park C, Jo WH. Adv Mater 2006;18:624.
[34] Yanf X, Hua F, Yamato K, Ruchenstein E, Gong B, Kim W, et al. Angew Chem Int Ed 2004;453:6471.
[35] Lohemeijer BGG, Schubert US. Angew Chem Int Ed 2002;41:3825.
[36] Pispas S, Floudas G, Pakula T, Lieser G, Sakellariou S, Hadjichristidis N. Macromolecules 2003;36:759.
[37] Bellomo EG, Wyrsta MD, Pakstis L, Pochan DJ, Deming T. Nat Mater 2004;3:244.
[38] Peng J, Xuan Y, Wang HF, Li BY, Han YC. Polymer 2005;46:5767.
[39] Sidorenko A, Tokarev I, Minko S, Stamm M. J Am Chem Soc 2003;125:12211.
[40] Zhao B, Haasch RT, Maclaren S. Polymer 2004;45:7979.
[41] Ma Y, Cao XY, Feng XJ, Ma YM, Zou H. Polymer 2007;48:7455.
[42] Fu Y, Bai S, Cui S, Qiu D, Wang Z, Zhang X. Macromolecules 2002;35:9451.
[43] Hwang J, Huh J, Jung B, Hong JM, Park M, Park C. Polymer 2005;46:9133.
[44] Zhao J, Jiang S, Ji X, An L, Jiang B. Polymer 2005;46:6521.
[45] Caricchi KA, Berthianme KJ, Russell TP. Polymer 2005;46:11635.
[46] Zhang Z, Wang Z, Xing R, Han Y. Polymer 2003;44:3737.
[47] Kim SH, Misner MJ, Xu T, Russell TP. Adv Mater 2004;16:226.
[48] Choy TC. Effective medium theory. New York: Oxford University Press; 1999.
[49] Ulmeanu M, Serghei A, Mihailescu IN, Budau P, Enachescu M. Appl Surf Sci 2000;165:109.